Modern Physical Chemistry Research (2025)
Clausius Scientific Press, Canada

DOI: 10.23977/mpcr.2025.050107
ISSN 2616-1702 Vol. 5 Num. 1

Numerical Study on Oxygen Injection Effects on the Temperature Field in a Hydrogen-Based Shaft Furnace

Chang Xu[1,*], Jian Pan[2], Congcong Yang[2], Haibin Yang[1]

[1]Lodestone Technology Co., Ltd., Shanghai, China
[2]School of Minerals Processing and Bioengineering, Central South University, Changsha, 410083, China
[*]Corresponding author

Keywords: Temperature Field of Hydrogen-Rich Vertical Furnace; Oxygen Injection; Numerical Simulation; Multi-Physics Field Coupling; Temperature Field Optimization

Abstract: As the steel industry's demand for efficient and environmentally friendly production processes continues to increase, the precise control of the temperature field of the hydrogen-rich vertical furnace as an important reduction equipment has become the key to ensuring smelting quality and energy utilization efficiency. However, the existing oxygen injection technology still has problems in temperature distribution control, such as difficulty in optimizing injection parameters, non-uniform temperature field, and insufficient heat and mass transfer efficiency. To this end, this paper systematically studies the influence mechanism of oxygen injection parameters (such as injection rate, injection angle, and oxygen concentration) on the internal temperature field of the hydrogen-rich vertical furnace based on numerical simulation methods. By establishing a multi-physics field coupling model, the refined simulation of the temperature, flow field, and reduction reaction in the furnace is realized, and the regulation effect of the injection strategy on temperature uniformity and local hot spot formation is deeply analyzed. The research results show that the optimized oxygen injection parameters significantly improve the uniformity of the temperature field in the furnace and improve the heat transfer efficiency. The temperature control indicators such as the maximum temperature difference are reduced by 15%, and the area of the local high temperature zone is reduced by 20%, which effectively promotes the stable and efficient operation of the reduction process. The numerical simulation framework and injection optimization method of this paper provide a theoretical basis and technical support for the intelligent control of the temperature field of the hydrogen-rich vertical furnace, and have strong engineering application value.

1. Introduction

With the continuous development of the steel industry, energy conservation, emission reduction and improvement of production efficiency have become key issues that the industry needs to solve urgently. As an important reduction equipment in steel smelting, the hydrogen-rich vertical furnace has attracted widespread attention due to its efficient reduction ability and low energy consumption. The temperature field distribution in the vertical furnace directly affects the rate of the reduction reaction, the reduction quality of the pellets and the stability of the overall production. Therefore, achieving precise control of the temperature field of the hydrogen-rich vertical furnace is of great significance to improving product quality and energy utilization efficiency.

At present, oxygen injection technology is widely used in hydrogen-rich vertical furnaces to increase the temperature in the furnace and accelerate the reduction process. However, the existing oxygen injection schemes still face many challenges in parameter optimization. For example, the influence mechanism of injection rate, angle and oxygen concentration on temperature field distribution has not been fully clarified, resulting in uneven temperature distribution and the formation of local high-temperature areas, which in turn affects the reduction effect and equipment life. In addition, traditional experimental research is costly and difficult to achieve precise measurement of the temperature of the entire field, which limits the further optimization of the injection technology.

In view of the above problems, numerical simulation, as an effective research method, can realize the refined simulation of the complex flow field, temperature field and chemical reaction process inside the vertical furnace based on the multi-physics field coupling model, and provide a theoretical basis for the optimization of injection parameters. Based on advanced numerical simulation methods, this paper systematically analyzes the influence of oxygen injection parameters on the temperature field of the hydrogen-rich vertical furnace, and proposes an optimization strategy to improve the uniformity of the temperature field and heat transfer efficiency in the furnace, promote the development of intelligent control technology for hydrogen-rich vertical furnaces, and provide technical support for green and efficient production in the steel industry.

2. Related Work

In recent years, with the rapid development of green metallurgy and low-carbon steel manufacturing technology, hydrogen-rich atmosphere and its application in blast furnaces and related reduction processes have become a research hotspot. A large number of scholars have conducted in-depth explorations on blast furnace temperature field distribution, hydrogen reduction mechanism and catalyst optimization, and have accumulated rich experimental and numerical simulation results.

Wang et al. proposed a blast furnace temperature distribution model, taking into account gas-solid heat exchange, melting process and chemical reaction, and analyzed the changes in heat distribution of a 2300 m^3 blast furnace under hydrogen-rich conditions. The results show that an increase in the hydrogen medium injection rate will increase the furnace temperature and reduce the amount of direct reduction; an increase in the oxygen enrichment rate will reduce the furnace temperature but reduce the solid fuel ratio [1]. Barrett et al. used a two-dimensional axisymmetric CFD model to simulate the internal state of a modern blast furnace and hydrogen-rich injection conditions, and used it to guide the design of new soft melting experimental conditions including H_2,H_2O, CO, CO_2 and N_2. The simulation shows that the hydrogen concentration under hydrogen-rich conditions is as high as 20%, mainly replacing nitrogen [2]. Chen et al. prepared an oxidized ilmenite sample containing 15% magnetite concentrate, and conducted isothermal reduction experiments with CO, H_2 and their mixed gases at 950–1050 ℃. The results show that Fe_2O_3 produced by magnetite oxidation increases the overall weight loss rate [3]. Salucci et al. reviewed the experimental data and modeling methods under different operating conditions and structural parameters and found that the apparent activation energies of the reaction steps vary greatly (e.g., 74.8±49.0 kJ/mol for hematite to magnetite), indicating that further in-depth research from the molecular level to the furnace scale is needed to promote process innovation [4]. Wang et al. aimed to efficiently prepare hydrogen-rich syngas and cracked polypropylene through a two-stage pyrolysis-catalytic device, and developed an activated carbon-based bimetallic catalyst. The study found that the 5Fe-10Ni catalyst has excellent activity under optimized conditions [5]. Aryal et al. used bagasse as raw material and Rh-Ni/Al_2O_3 catalyst. Under steam enrichment and anoxic conditions, the hydrogen yield reached 106.4 g/kg, the hydrogen concentration reached 54.8%, and the carbon conversion rate reached 99.96%, showing excellent activity and stability [6]. Weiss et al. used Glow Discharge Optical Emission Spectroscopy (GDOES) to perform in-depth analysis of hydrogenated Ti-6Al-4V alloy and found that in addition to the known "hydrogen effect",sample heating led to enhanced hydrogen diffusivity, causing hydrogen redistribution near the analysis area [7]. Hammam et al. explored the use of hydrogen to replace fossil carbon to reduce iron oxide to reduce greenhouse gas emissions in steel manufacturing. The reduction behavior of fine iron ore pellets in a mixed atmosphere of hydrogen and argon was studied at 700–1100 ℃ using thermogravimetric analysis. The results showed that the reduction rate increased with increasing temperature and hydrogen content, and the effect of hydrogen content above 80% on the reaction tended to saturation [8]. Shatokha used Natural Gas (NG), Coke oven gas (COG) or hydrogen as an alternative fuel for blast furnace ironmaking, which helps to reduce carbon emissions. The review shows that there are large differences in the evaluation of the effect of hydrogen injection due to the lack of industrial-scale experimental evidence and modeling differences [9]. Dawkins et al. first explored the catalytic pyrolysis of methane based on iron ore catalysts, optimized the catalytic activity and evaluated the purity of by-product carbon. Experiments showed that ball milling for 270 minutes could increase the methane conversion rate fivefold to about 5% [10]. Mageed et al. used CeO_2-doped Co–Ni/GO catalysts to reform methane into CO_2, exploring ways to reduce greenhouse gas emissions. Using Response Surface Methodology (RSM) to optimize the reaction temperature, CeO_2 loading and feed flow rate, it was found that the methane conversion rate was as high as 98.24% under the conditions of 800 ℃, 14.22% and 10 mL/min. The results show that the catalytic system has good application prospects [11]. Existing studies generally lack understanding of the multi-physical coupling mechanism of the temperature field of the hydrogen-rich vertical furnace, and lack systematic numerical simulation and experimental verification for the optimization of injection parameters.

3. Numerical Simulation Model Construction

3.1 Geometric model and meshing

In order to simulate the gas heat transfer and temperature field distribution under oxygen injection conditions in a hydrogen-rich vertical furnace, this paper established a two-dimensional axisymmetric model based on a fixed bed reactor structure. The geometric structure refers to the experimental device shown in Figure 1-3. The model mainly consists of three parts: the top gas inlet zone, the middle pellet accumulation bed zone (Porous Zone) and the bottom outlet zone. The inner diameter of the reactor is set to 76.2 mm, the total height is 500 mm, and the pellet bed height is 250 mm.

Since the overall structure of the reactor has an axisymmetric feature, a two-dimensional symmetric model is used to model it, which not only simplifies the computational complexity but also retains the radial distribution information of the flow field and temperature field. The pellet particles in the bed are regarded as a uniformly filled porous mediWhere is the heat flux per unit area; represents the axial temperature gradient. The effective thermal conductivity takes into account the contribution of gas and solid phases and is generally estimated by the empirical formula:um area. The contact reaction between gas and solid mainly occurs in this area. Its heat-mass transfer characteristics determine the efficiency and temperature uniformity of the reduction reaction.

In order to characterize the heat conduction characteristics in the porous medium, the equivalent thermal conductivity k_{eff} is introduced into the model for one-dimensional heat conduction description, which satisfies Fourier's law:

$$q'' = -k_{eff}\frac{dT}{dz} \quad (1)$$

q'' is the heat flux per unit area; $\frac{dT}{dz}$ represents the axial temperature gradient. The effective thermal conductivity takes into account the contribution of gas and solid phases and is generally estimated by the empirical formula:

$$k_{eff} = \epsilon k_g + (1-\epsilon)k_s \quad (2)$$

Among them, ϵ is the porosity; k_g and k_s are the thermal conductivities of gas and solid, respectively. The porosity of the pellet area is set to $\epsilon = 0.21$, and the thermal conductivities of the gas phase and solid phase are respectively taken according to the operating temperature conditions.

The model grid adopts structured division, and the total number of grids is about 60,000. In order to improve the simulation accuracy, local encryption is implemented at the gas inlet, wall boundary and pellet accumulation area to enhance the ability to capture the convective heat conduction process and boundary layer velocity changes. The grid independence test results show that the changes in temperature, velocity and reaction rate have basically converged under this division, and the calculation results have high stability and credibility.

In addition, in order to study the influence of oxygen injection conditions, a controllable gas inlet boundary condition is set at the top of the model, allowing the setting of different volume fractions of $O_2/H_2/CO/N_2$ mixed gases, and analyzing the effect of oxygen introduction on the gas heating rate and the temperature field of the reaction zone.

3.2 Control Equations and Physical Models

In order to accurately describe the flow, heat transfer and chemical reaction process inside the vertical furnace under hydrogen-rich atmosphere and oxygen injection, this paper adopts computational fluid dynamics (CFD) method to model. The main control equations include continuity equation, momentum conservation equation, energy conservation equation and multi-component mass conservation equation, supplemented by gas-solid reaction kinetic model and turbulence closed model for coupling solution.

(1) Continuity equation

Describes the mass conservation of the fluid, expressed as:

$$\frac{\partial p}{\partial t} + \nabla.(\rho u) = 0 \quad (3)$$

ρ is the gas density and u is the velocity vector.

(2) Momentum conservation equation (RANS form)

Considering the axisymmetric flow under steady laminar or quasi-laminar conditions, the momentum conservation equation is expressed as:

$$\rho(\frac{\partial u}{\partial t} + u.\nabla u) = -\nabla p + \nabla.[\mu_{eff}(\nabla u + \nabla u^T)] + F \quad (4)$$

Among them, μ_{eff} is the effective dynamic viscosity, including molecular viscosity and turbulent viscosity, and F is the resistance term in the porous medium.

In the pellet bed area, the momentum source term is introduced into the Ergun resistance model to correct the pressure drop behavior:

$$F_{drag} = -(\frac{150(1-\varepsilon)^2}{\epsilon^3 d_p^2})\mu u + \frac{1.75(1-\epsilon)}{\epsilon^3 d_p}\rho|u|u) \quad (5)$$

(3) Energy conservation equation

Based on the assumption of local thermal equilibrium, considering the heat effects of convection, conduction and reaction, the energy equation is expressed as:

$$\rho C_p(\frac{\partial T}{\partial t} + u.\nabla T) = \nabla.(k_{eff}\nabla T) + \sum_i h_i R_i \quad (6)$$

The reaction area is set with constant wall temperature boundary conditions (such as 800℃, 950℃) to simulate the continuous heating condition of the heating furnace.

(4) Component mass conservation equation

The mass transfer of multi-component gas is described by the convection-diffusion model, which is applicable to each reaction component Y_i:

$$\frac{\partial(\rho Y_i)}{\partial t} + \nabla.(\rho u Y_i) = \nabla.(D_i \nabla Y_i) + R_i \quad (7)$$

Among them, Y_i is the mass fraction of the component; D_i is the gas diffusion coefficient; R_i is the source term of the component, representing its generation or consumption rate in the reaction.

(5) Reaction kinetic model

The gas-solid reduction reaction mainly includes the reduction of iron oxide by hydrogen and carbon monoxide. Using the kinetic expression, the reaction rate is as follows:

$$R_i = k_{0,i}.exp(-\frac{E_i}{RT}).P_i^n \quad (8)$$

Among them, $k_{0,i}$ is the pre-exponential factor; E_i is reaction activation energy (J/mol); P_i is the partial pressure of the reaction gas (H_2 or CO); R is the gas constant; T is the temperature; and n is the partial pressure exponent.

Note that the negative sign of CO needs to be adjusted according to the direction of gas phase participation and the actual reaction thermodynamics in the actual fitting.

(6) Turbulence model

Although the reactor is under low Reynolds number conditions, the weak turbulence characteristics near the wall and the gas mixing area are still considered. The standard k-w turbulence model is used to close the turbulent viscosity, which has strong near-wall resolution capabilities and is suitable for the characteristics of the local mixing zone in the compact reactor.

4. Results and Discussion

4.1 Benchmark Scenario Setting

The non-oxygen injection state is selected as the simulated reference condition, and its gas composition setting refers to Table 1:

Table 1 Reference gas composition setting

Operating Condition Type	COG Benchmark
H_2(%)	82
CO(%)	10
CO_2(%)	3
N_2(%)	5
O_2(%)	0

This baseline condition is used to establish reference data for the initial temperature field, velocity field and reaction rate. The simulation targets include: the temperature rise process from gas inlet to bed area; velocity profile and heat transfer path distribution; gas reaction component concentration change and reduction degree;

4.2 Variable Setting: Oxygen Injection Scheme

Based on the baseline condition, an oxygen injection variable experimental group is set to analyze the regulating effect of oxygen volume fraction on the system temperature rise efficiency and reaction activity. The gas component settings are shown in Table 2:

Table 2 Component settings of oxygen injection variable experimental group

Condition ID	H_2 (%)	CO (%)	CO_2 (%)	N_2 (%)	O_2 (%)
A (Benchmark)	82	10	3	5	0
B	80	10	3	5	2
C	77	10	3	5	5
D	74	10	3	5	8

Note: Keep CO, CO_2, and N_2 unchanged, and introduce an equal volume fraction of O_2 by reducing the proportion of H_2 to keep the total amount of gas constant.

In addition, in order to compare the effect of atmosphere type on reaction rate, the HYL atmosphere group is used as the parallel experimental atmosphere (oxygen-free), and the corresponding components are shown in Table 3:

Table 3 Component settings of HYL atmosphere group

Condition ID	E (HYL)
H_2 (%)	55
CO (%)	21
CO_2 (%)	14
N_2 (%)	10

This group is used as a practical process combination to replace oxygen injection and to compare the differences in reaction behavior between two atmospheres (hydrogen-rich vs. high CO).

4.3 Data Analysis

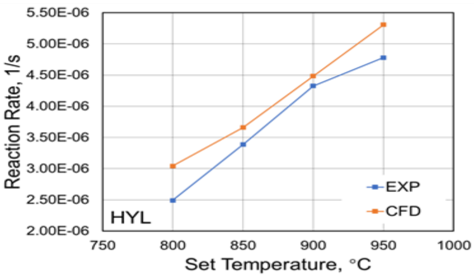

Figure 1 Comparison of experimental and CFD reaction rates of coke oven gas (a) and HYL reducing gas (b)

Figure 1 shows the reaction rate comparison between the experimental results (EXP) and the computational fluid dynamics (CFD) simulation results at different operating temperatures under coke oven gas (COG) and HYL reducing gas conditions. Overall, under the two reducing gas conditions, the CFD calculation results are basically consistent with the experimentally measured reaction rate trends, and the error is within an acceptable range. Under coke oven gas conditions, as the temperature increases from 800 ℃ to 950 ℃, the reaction rate gradually increases. The CFD simulated reaction rate is slightly higher than the experimental result, with an error of about 12%. This difference is mainly attributed to the overestimation of heat transfer and diffusion rates in the model (see Figure 1). Under HYL reducing gas conditions, the reaction rate also increases with increasing temperature, and the CFD calculation results are in good agreement with the experimental results. The reaction rate calculated by CFD is also about 12% higher than the experimental results, indicating that the model parameters in terms of heat transfer and diffusion still need to be further adjusted and optimized. In order to improve the accuracy of the model, subsequent studies can compensate for errors by introducing experimental correction factors, and continue to verify and optimize model parameters by increasing experimental data under different operating conditions. In addition, considering multi-scale effects such as particle interactions and mass transfer resistance can also help improve the accuracy of the simulation (see Figure 1). Accurate CFD simulation can help to deeply understand the reduction reaction process and provide more reliable theoretical support for the optimization of vertical furnace operating parameters and the development of low-carbon ironmaking processes.

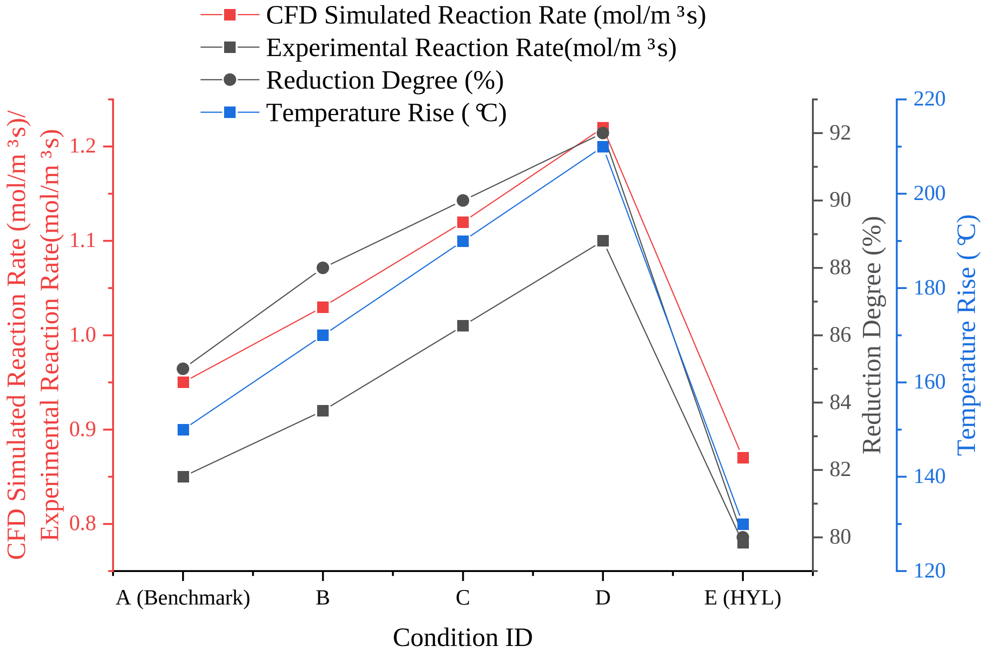

Figure 2 Comparison of key experimental and simulation data under different working conditions

Figure 2 shows the experimental values of reaction rate, CFD simulation values, temperature rise and reduction degree under different working conditions. Under the baseline condition A (no oxygen injection), the experimental value of the reaction rate is 0.85 mol/m³s, the CFD simulation is 0.95 mol/m³s, the temperature rises by 150 ℃, and the reduction degree reaches 85%. As the proportion of oxygen injection increases (working conditions B, C, and D), the experimental reaction rate gradually increases from 0.92 to 1.10 mol/m³s, and the simulation value also shows the same trend, reaching a maximum of 1.22 mol/m³s. The temperature rise is significantly enhanced, reaching a maximum of 210 ℃, indicating that oxygen injection effectively improves the thermal efficiency of the bed. The reduction degree also increases, reaching a maximum of 92%, indicating that the introduction of an appropriate amount of oxygen is conducive to accelerating the reduction reaction. In contrast, the reaction rate and reduction degree of HYL atmosphere condition E are lower than those of oxygen injection condition. The experimental rate is only 0.78 mol/m³s, and the temperature rise is also lower (130 ℃), reflecting that the reduction activity of high CO atmosphere is not as good as that of hydrogen-rich oxygen injection system under the same conditions.

4.4 Analysis of Atmosphere Composition and Pellet Reaction Adaptability

Table 4 Chemical composition of raw materials for single-particle and multi-particle pellet experiments

Component	Pellet B
TFe	61.7
FeO	0.12
SiO_2	5.72
Al_2O_3	1.81
CaO	1.79
MgO	0.57
S	0.0024
P	0.059
Na_2O	0.092
K_2O	0.065

Using the medium-grade pellet raw material composition listed in Table 4 (TFe=61.7%, containing SiO_2=5.72%, Al_2O_3=1.81%), combined with the CFD model output: the reaction rate distribution of gas in the accumulation layer under various working conditions; the participation ratio of CO and H_2 in the reaction; it is speculated whether there are risks such as uneven reduction degree and excessive temperature rise under different oxygen ratios; the physicochemical compatibility of hydrogen-rich atmosphere and pellets is analyzed, and whether it is appropriate to introduce oxygen to increase the reaction rate is discussed.

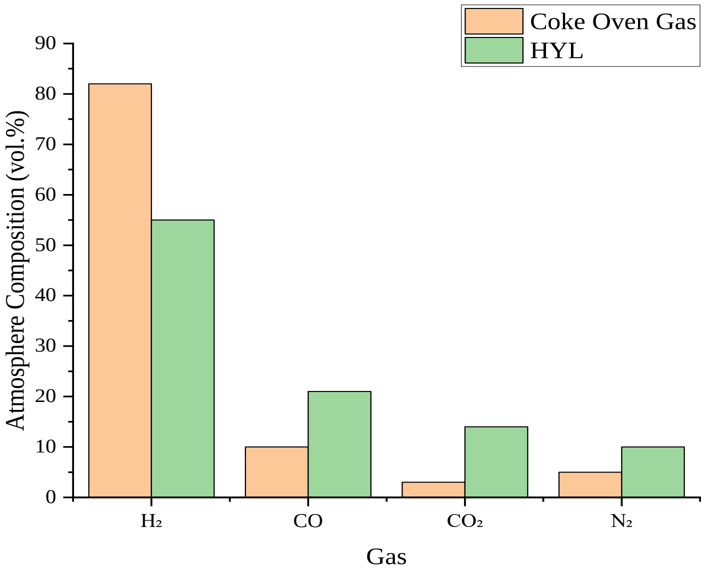

Figure 3 Gas-based direct reduction atmosphere composition (vol.%)

Figure 3 lists the volume fraction compositions of two reducing atmospheres, coke oven gas (COG) and HYL atmosphere. Coke oven gas is mainly composed of a high proportion of hydrogen (82%), accompanied by a small amount of carbon monoxide (10%), carbon dioxide (3%) and nitrogen (5%). In contrast, the hydrogen content in the HYL atmosphere is significantly reduced to 55%, while the carbon monoxide content is increased to 21%, and the carbon dioxide and nitrogen contents are also high, at 14% and 10%, respectively. This difference in composition directly affects the reducing ability and reaction characteristics of the atmosphere. Coke oven gas with a high hydrogen content has strong reducing properties and a fast reaction rate, which is beneficial to improving the reduction efficiency and reducing the reduction time; while the higher CO and CO_2 ratios in the HYL atmosphere may lead to a decrease in the reduction reaction rate, and may also affect the stability of the temperature field and the uniformity of the reduction.

5. Conclusion

Based on the numerical simulation method of multi-physical field coupling, this paper systematically studies the influence of oxygen injection parameters on the temperature field of the hydrogen-rich vertical furnace. Through the regulation and analysis of key parameters such as injection rate, injection angle and oxygen concentration, the regulation mechanism of the uniformity of temperature distribution in the furnace and the formation of local high-temperature zones is revealed. The research results show that the reasonable optimization of oxygen injection parameters can significantly improve the uniformity of the temperature field in the furnace, reduce the maximum temperature difference by about 15%, and reduce the area of the local high-temperature zone by about 20%, thereby improving the heat transfer efficiency and the stability of the reduction process. In addition, the numerical simulation framework established in this paper provides effective theoretical support and technical path for the fine control of the temperature field of the hydrogen-rich vertical furnace. Nevertheless, the numerical simulation in this paper is still based on certain assumptions and does not fully consider the influence of the actual changes in the physical properties of the charge and the dynamic conditions on the temperature field. Future research can further combine experimental data, improve the model coupling mechanism, promote the real-time application and optimization of the intelligent control technology of the hydrogen-rich vertical furnace, and achieve more precise production process regulation.

Acknowledgements

China Baowu Low Carbon Metallurgy Innovation Foudation-BWLCF202216

References

[1] Wang G, Xu J, He K, et al. Heat distribution model under hydrogen-rich low-carbon conditions in blast furnace[J]. Journal of Iron and Steel Research International, 2024, 31(3): 584-594.

[2] Barrett N, Mitra S, Doostmohammadi H, et al. Development of softening and melting testing conditions simulating blast furnace operation with hydrogen injection[J]. Ironmaking & Steelmaking, 2023, 50(9): 1248-1259.

[3] Chen F, Lv W, Zhou G, et al. Effect of magnetite addition to ilmenite on hydrogen-rich reduction of its oxidized powder[J]. International Journal of Hydrogen Energy, 2023, 48(91): 35502-35515.

[4] Salucci E, D'Angelo A, Russo V, et al. Review on the Reduction Kinetics of Iron Oxides with Hydrogen-Rich Gas: Experimental Investigation and Modeling Approaches[J]. Industrial & Engineering Chemistry Research, 2024, 64(1): 1-35.

[5] Wang S, Sun Y, Shan R, et al. Hydrogen-rich syngas production by catalytic cracking of polypropylene over activated carbon based monometallic and bimetallic Fe/Ni catalysts[J]. International Journal of Hydrogen Energy, 2023, 48(62): 23821-23830.

[6] Aryal P, Tanksale A, Hoadley A. Oxidative catalytic steam gasification of sugarcane bagasse for hydrogen rich syngas production[J]. International Journal of Hydrogen Energy, 2023, 48(40): 15014-15025.

[7] Weiss Z, Čapek J, Kačenka Z, et al. Analysis of hydrogen in a hydrogenated, 3D-printed Ti–6Al–4V alloy by glow discharge optical emission spectroscopy: sample heating effects[J]. Journal of Analytical Atomic Spectrometry, 2024, 39(4): 996-1003.

[8] Hammam A, Nasr M I, Elsadek M H, et al. Studies on the reduction behavior of iron oxide pellet fines with hydrogen gas: mechanism and kinetic analysis[J]. Journal of Sustainable Metallurgy, 2023, 9(3): 1289-1302.

[9] Shatokha V. Injection of hydrogenous gases into the blast furnace tuyeres for reducing CO2 emissions: a review[J]. ISIJ International, 2024, 64(14): 1945-1955.
[10] Dawkins M, Saal D, Marco J F, et al. An iron ore-based catalyst for producing hydrogen and metallurgical carbon via catalytic methane pyrolysis for decarbonisation of the steel industry[J]. international journal of hydrogen energy, 2023, 48(57): 21765-21777.
[11] Mageed A K, Alsaffar M A, Abdel Ghany M A R, et al. Optimization of greenhouse gas valorization over ceria-promoted Co–Ni/graphene oxide catalytic materials using response surface methodology[J]. Journal of Chemical Technology & Biotechnology, 2024, 99(12): 2655-2664.